Landscape & Environment 7 (2) 2013. 74-80.

IN-FLIGHT ICING CHARACTERISTICS OF UNMANNED AERIAL VEHICLES DURING SPECIAL ATMOSPHERIC CONDITION OVER THE CARPATHIAN-BASIN

ZSOLT BOTTYÁN

National University of Public Service, Department of Military Aviation
Hungary, 5000, Szolnok, Kilián u. 1.
University of Debrecen, Department of Meteorology
Hungary, 4032, Debrecen, Egyetem tér 1.
E-mail: bottyan.zsolt@uni-nke.hu

Received 19 december 2013, accepted in revised form 16 january 2013

Abstract
The in-flight aerial icing phenomena is very important for the Unmanned Aerial Vehicles (UAV) because it causes some serious problems such as reduced lift and increased drag forces, significantly decreased angle of attack, increased weight, structural imbalances and improper radio communications. In order to increase flight safety of UAV's we develop an integrated meteorological support system for the UAV pilots, mission controllers and decision makers, too. In our paper we show the in-flight structural icing estimation method as a part of this support system based on a simple 2D ice accretion model predictions. We point out the role of the ambient air temperature, cloud liquid water content, airfoil geometry and mainly the true airspeed in the icing process on the wings of UAVs. With the help of our model we made an estimation of geometry and amount of ice accretion on the wing of a short-range and a high-altitude and long-endurance UAVs during a hypothetical flight under a typical icy weather situation with St clouds over the Carpathian-basin (a cold-pool situation case study). Finally we point out that our icing estimation system can easily be adapted for supporting the missions of UAVs.

Keywords: unmanned aerial vehicle, UAV, structural icing, cold-pool situation, icing prediction, meteorological support

1. Introduction

The accreted ice layer causes many dangerous problems during the flight such as reduced lift and increased drag forces, significantly decreased the angle of attack, strong vibrations and structural imbalances of UAVs, malfunction of control surfaces and air pressure sensors, reduced visibility and improper radio communication (Gent et al. 2000; Bragg et al. 2005).

Generally the UAVs are not equipped with any anti-icing possibilities thus these planes cannot remove the accreted ice layers during the flight. On the other hand the weight of developed ice layers in the case of UAVs is the stronger effect than the manned ones because the UAVs have usually smaller maximum take-off weigth (MTOW). Furthermore the UAVs have generally been built with a special wing profiles with high curvature of their leading edge. It follows the collision efficiency of these wings are very high during the flight in the icy circumstances like in Cb, Ns and St clouds as well (Makkonen – Stallabrass 1987; Mazin et al. 2001).

On the other hand during the winter half-year the atmosphere often produces different weather situations with significant icing conditions over the Carpathian-basin which are absolutely hazardous states for the UAVs flights. The more important cases are the followings:

- the summer half year thunderstroms with huge Cb clouds,
- the warm frontal Ns clouds with large horizontal and vertical extension and
- winter half-year anticyclonic cold-pool

situation with vertically thin but horizontally wide St clouds.

We have to note two other dangerous in-flight icing states can happen outside of clouds during the flight caused by freezing rain and freezing drizzle precipitations (Fuchs – Schickel 1995; Bernstein 2000). These latter icing types are not discussed in our work.

In order to prevent the UAVs, their pilots and mission specialists from undesirable weather impacts we develop an integrated meteorological support system (IMSS) for the mentioned crew persons. This support system contains a statistical and dynamical weather prediction unit based on 3D meteorological measurements to product an efficient combined weather prediction for ensure of the UAV missions (Hansen 2007; Bottyán et al. 2013). Of course the given model outputs are post processed with the special regard to dangerous weather phenomena such as icing, turbulence, low visibility, etc.

In our paper we show the in-flight structural icing estimation method and its ice layer predictions in connection with a hazardous atmospheric situation over the Carpathian Basin.

2. 2D Ice accretion model

Forecasting of airframe (structural) icing of UAVs is a very complex procedure and the rate and amount of structural ice accretion curiously depend on the followings (Gent et al. 2000; Lankford 2001):

- static ambient temperature of airflow around the UAV,
- static air pressure at the level of flight,
- liquid water content (LWC) of cloud,
- cloud droplet size distribution,
- true airspeed (TAS) of UAV and
- shape and size of UAV structures with the special regard to its wings.

The applied ice accretion model is based on the quasi-stationary heat balance equation Eq. (1) for a freezing surface which is assumed to define the thermodynamics of icing phenomena, described in detail earlier (Ludlam 1951; Messinger 1953; Lozowski et al. 1983a; Finstad et al. 1988; Mazin et al. 2001; Szilder – McIlwain 2011).

$$Q_c+Q_e+Q_v+Q_k+Q_f+Q_w+Q_i+Q_r+Q_w^*+Q_f^*=0 \quad (1)$$

where

- Q_c – is the sensible heat flux between freezing surface and airstream;
- Q_e – is the latent heat flux of evaporation;
- Q_v – is the viscous aerodynamic heating due to airstream;
- Q_k – is the flux of kinetic energy of impinged droplets on the icing surface;
- Q_f – is the latent heat flux of accretion due to freezing of impinging water;
- Q_w – is the sensible heat flux required to warm the freezing water droplets;
- Q_i – is the heat flux between the iced and the underlying surface;
- Q_r – is the long-wave radiative heat flux;
- Q_w^* – is the sensible heat flux required to heat the runback and shedding part of impinging water (similar to Q_w);
- Q_f^* – is like Q_f but for runback water only.

However, this approach is based on Eq. (1) can be applied to estimate the ice accretion rate if we use a short time interval which is not longer than 5–7 minutes (Bottyán 2011). On the other hand the shapes of accreted ice contamination grew during the wind tunnel experiments are very similar to those calculated by the applied ice growth model. These experiments were executed under conditions such as –5 °C and –15 °C temperature, 30.5 – 122 m/s true airspeed (TAS), 0.13 – 1.27 g/kg LWC and 1 – 10 minutes time intervals, respectively (Lozowski et al., 1983b).

Because of the above mentioned model predicts the accreted ice layers along a non-rotating cylinder surface we had to determine the curvature radius of the leading edge in the case of examined UAVs which is based on the work of Tsao and Anderson (2005).

3. The examined UAVs

In this study we examine two UAVs to

demonstrate the appearing different ice accretion during a special icy environmental (meteorological) conditions over the Carpathian basin.

The smaller one is the ELBIT Skylark-I LE SUAV as it can be seen in Fig. 2. This airplane is used by some military units e.g. by Hungarian Army. It has relative small operational distance and height but simple and economic SUAV thus they are generally applied in the shorter reconnaissance missions.

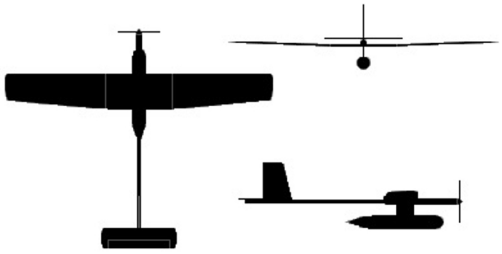

Fig. 1. The ELBIT Skylark-I LE SUAV. Source: http://hu.m.wikipedia.org/w/index.php?title=F%C3%A1jl:Skylark_1.jpg&filetimestamp=20070519131044

The airfoil of Skylark-I LE is the Roncz Low Drag airfoil which has about 0.3m chord length thus the corresponding cylinder diameter is 0.0105 m at the leading edge (Abbott – Doenhoff 1959). The examined true airspeeds of this SUAV were 20 m/s and 30 m/s. (Fig. 3.)

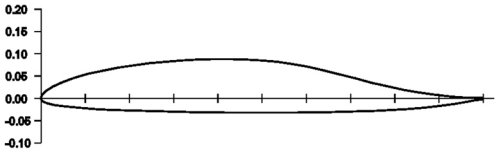

Fig. 2. The Roncz Low Drag airfoil applied on the ELBIT Skylark-I LE SUAV. Source: http://www.airfoildb.com/foils/showplot/490

The other examined airplane is the Northrop Grumman RQ-4 Global Hawk Block 30 UAV can be seen in Fig. 4. This UAV is a high altitude and long endurance (HALE) unmanned airplane which has the NASA LRN 1015 airfoil with the chord length of 1.6m and the corresponding cylinder diameter of 0.0704 m at its leading edge (Abbott and Doenhoff, 1959). The RQ-4 works in a wide range of airspeed and height intervals alike so we studied the airspeeds between 50 m/s and 130 m/s (Fig. 5).

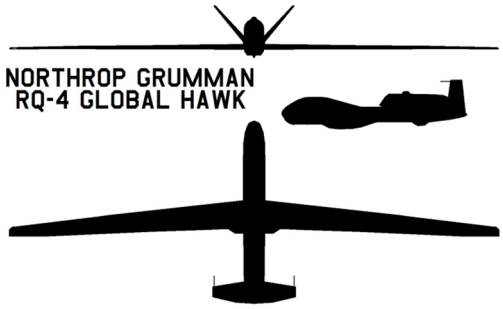

Fig. 3. Northrop Grumman RQ-4 Global Hawk Block 30 HALE UAV. Source: http://fc05.deviantart.net/fs47/f/2009/185/9/2/Northrop_RQ_4_Global_Hawk_by_bagera3005.png

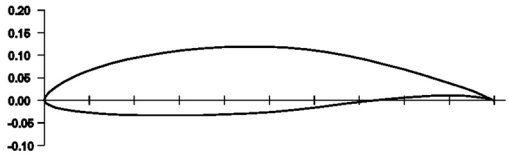

Fig. 4. The NASA NLF 1015 airfoil which is very similar to NASA NLR 1015 one which is applied on Global Hawk. Source: http://www.airfoildb.com/foils/showplot/281

4. A case study

In order to study the icing characteristics of the mentioned UAVs we examined a special icy weather situations over the Carpathian-basin. In January 22, 2006 there was a wide, low and cold St cloud over the Carpathian-basin which is so called "cold-air pool formation" (Iijima – Shinoda 2000). As we can see in figure 5 there was a significant anticyclonic state over the Central-Europe region with the special regards to the Carpathian-basin, too. The highest sea level pressure was 1049 hPa next to the examined geographical region. The environmental condition was favorable to in-flight icing inside the low St cloud because the temperature was below zero in it and the mentioned cloud contained a large amount of supercooled cloud droplets with the Γ-size distribution (Kunkel 1971; Jeck

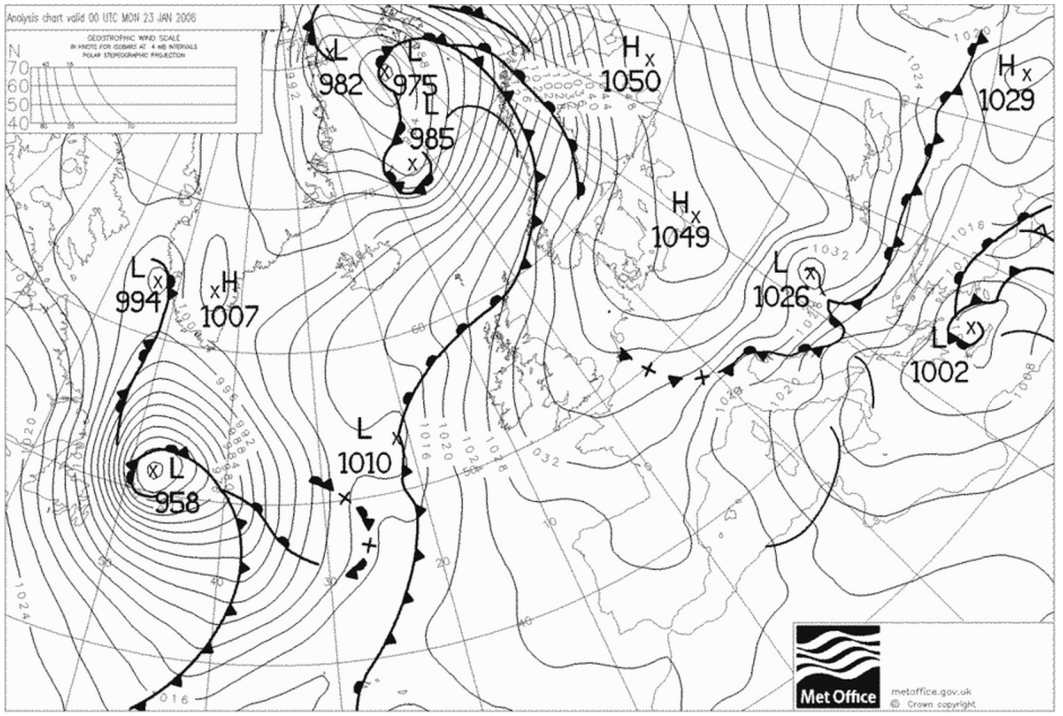

Fig. 5. The european weather situation at 00UTC in January 22, 2006. Source:http://www.wetterzentrale.de/topkarten/tkfaxbraar.htm

2002). We have to note the similar weather situations can often be observed during the winter season in the mentioned region thus the examination this atmospheric states and its phenomena essentially important in aviation meteorology, too.

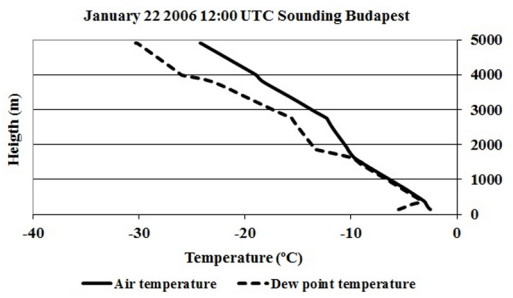

Fig. 6. The temperature and dew point temperature profile over Budapest in January 22, 2006 at 12:00 UTC. Source: http://weather.uwyo.edu/upperair/europe.html

Supposing the LWC was a constant value of 0.5 g/kg in the mostly homogenous cloud, the hypothetical flying height and duration were 600 m (at the 950 hPa pressure level) and 5 minutes, respectively. On the other hand at the flying level the ambient air temperature, the dew point temperature and relative humidity were observed by radio sounding with the following values: –4.2 °C, –4.5 °C and 98% (Fig. 6).

5. Results and discussion

First of all, we calculated the ice accumulation and its rate along the airfoil (cylinder) surface of the Global Hawk UAV under the given meteorological conditions at 12 UTC on January 22, 2006 over Budapest. The applied true airspeeds (TAS) were 50 m/s and 100 m/s.

As we can be seen on the left side of Fig. 7 during the mentioned hypothetical flight (with 50 m/s TAS) over the Carpathian-basin, the accreted ice shape shows us the icing condition was slightly wet because the

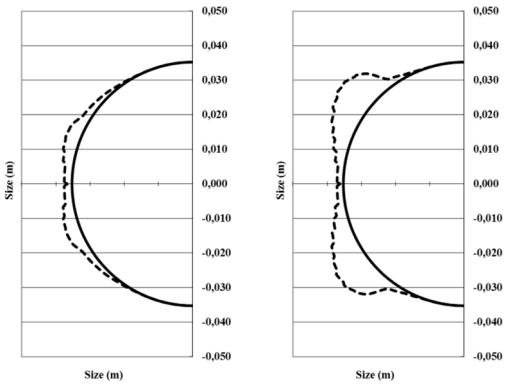

Fig. 7. The 2D geometry of computed accreted ice layers on the surface of the given cylinder (airfoil) of the Global Hawk UAV after 5 minutes flight time. T= –4.2 °C; p = 950 hPa; LWC = 0.5 g/kg; Left: TAS= 50 m/s. Right: TAS= 100 m/s. The blue line shows the ice accretion geometry and the brown one represents the surface of airfoil itself

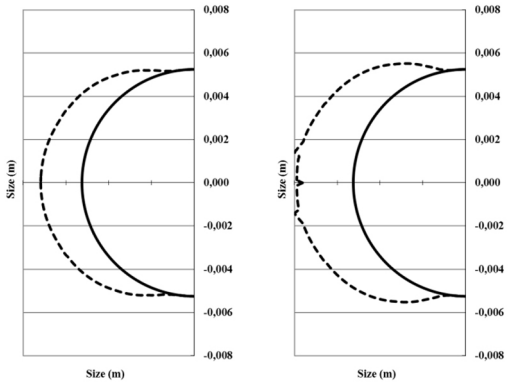

Fig. 8. The 2D geometry of computed accreted ice layers on the surface of the given cylinder (airfoil) of the Skylark-I SUAV after 5 minutes flight time. T= –3.0 °C; p = 1010 hPa; LWC = 0.5 g/kg; left: TAS= 10 m/s. Right: TAS= 20 m/s.

maximum ice thickness was not found at the leading edge exactly. The maximum rate of this icing was 0.85 mm/min which meant moderate intensity on the international standards of Federal Aviation Administration (FAA) icing severity scale given by Jeck (1998), which are similar to ICAO ones.

As we applied the 100 m/s TAS, the geometry of accreted ice highly changed, formed a very dangerous horn-ice shape layer because the environmental conditions led a strong wet icing (Fig. 7, right). In this case the calculated 2.02 mm/min maximum ice accretion rate was equal severe FAA icing intensity. On the other hand the 2.02 mm/min predicted maximum ice accumulation rate means the 10.1 mm thick maximum accreted ice layer during 5 minutes flight under these conditions. This procedure results about 9.09g weight ice on every square cm along the wings of Global Hawk at 35 degree from leading edge (where the accumulation was the highest).

Under the the same examined atmospheric state ("cold pool situation") over the Carpathian basin with the Skylark-I LE SUAV showed the exact dry icing situation if the flight was as slow as 20 m/s TAS (Fig. 8 left). In this case the maximum ice accumulation area was located at the leading edge with a maximum value of 0.39 mm/min which meant a light icing severity according to FAA scale.

When we changed the TAS from 20 to 30 m/s the icing characteristics varied and formed a little horn-like ice layer which meant the wet icing conditions (Fig. 8 right). The maximum value of the rate of ice accretion was 0.63 mm/min and it appeared at 10 degree from leading edge and it was a moderate FAA icing severity, in this case.

As it can be seen in the above mentioned part of our work the true airspeed (TAS) is a very important factor in airframe icing processes.

Demonstrating this effect we show our Global Hawk ice accretion calculations under the same applied meteorological situation with the different true airspeed values from 70 m/s up to 130 m/s. When the true airspeed matched 70 m/s the shape of the predicted ice layer had been strongly formed with its horns as the icing procedure was basically wet (Fig. 9. left). With increasing of true airspeed (TAS=90 m/s) the ice layer geometry was changing toward the significant horn-like ice accretion on the UAV wing (Fig. 9. right). In this case we could be observed a more

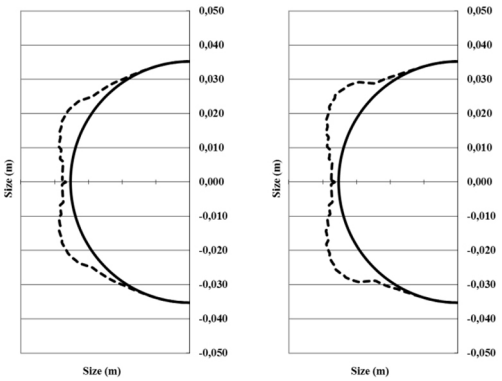

Fig. 9. The 2D geometry of computed accreted ice layers on the surface of the given cylinder (airfoil) of the Global Hawk UAV after 5 minutes flight time. T= –4.2 °C; p = 950 hPa; LWC = 0.5 g/kg; Left: TAS= 70 m/s. Right: TAS= 90 m/s.

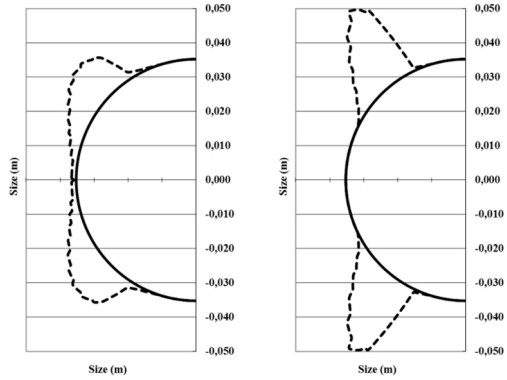

Fig. 10. The 2D geometry of computed accreted ice layers on the surface of the given cylinder (airfoil) of the Global Hawk UAV after 5 minutes flight time. T= –4.2 ºC; p = 950 hPa; LWC = 0.5 g/kg; Left: TAS= 110 m/s. Right: TAS= 130 m/s. The blue line shows the ice accretion geometry and the brown one represents the surface of airfoil itself

significant ice layer with a large flat area has a larger drag force. At 110 m/s true airspeed the accretion has essentially a typical horn-like shape geometry with a larger shadow zones beneath the ice horns (Fig. 10 left). On the other hand between 110 m/s and 130 m/s TAS the attribute of accreted layer had dramatically been changed because of the distribution of ice contamination. The maximum value of the rate of ice accretion was 8.88 mm/min and it appeared at 56 degree from leading edge and it was a highly severe FAA icing severity, in this case.

As long as the geometrical effects of UAVs are initially constants, the atmospheric parameters may vary along wide ranges in the clouds during the flight with the special regards to convective ones such as Cb and Cu cong. It follows that the provision of a responsible quasi real-time prediction in the matters of rate, amount, and geometry of airframe ice accretion requires the good knowledge of meteorological (cloud microphysical) conditions and flight plan (airspeed, duration, and 3D route of flight), together. The necessary high resolution values of signed meteorological variables can be produced by a meso-scale numerical weather model such as WRF with a corresponding parameterization (Skamarock et al. 2005).

It is clear the examined weather situation involves a highly dangerous in-flight icing phenomena for UAVs during their flight over the Carpathian-basin. The showed model and its applying in our IMSS system with a WRF numerical model implementation give a good chance to predict the in-flight icing severity more exactly in the future (Bottyán et al. 2013). Based on our development we hope the military and civil aviation safety will be more higher over the whole Carpathian-basin because predicting well the flight environment, we may derive a maximum flight time for a given UAV during this situation without any dangerous icing (flight path optimization).

6. SUMMARY

On the basis of the described model and our results, we are able to estimate the exact icing rate and geometry on the wings of a given UAV during a relatively short time period. There is also a good advantage to calculate the correct limits of the icing severities regarding to given meteorological, aerodynamical and geometrical conditions

(aircraft-dependent estimations). Applying the calculated geometry (shape) of the accreted ice layer, we are able to predict the most dangerous horn-iced phenomena and its probable location within the cloud. Moreover, the embedding of a similar ice accretion model (such as described one) into an operative forecasting procedure can level up the usage and reliability of icing predictions and may lead to higher level of flight safety.

Acknowledgement

This work was supported by the European Social Fund (TÁMOP-4.2.1.B-11/2/KMR-2011-0001 and the TÁMOP-4.2.2.C-11/1/KONV-2012-0010 projects).

7. REFERENCES

Abbott, I. H. – von Doenhoff, A. E. (1959): Theory of Wing Sections. Dover, New York.

Berstein, B. C. (2000) Regional and Local Influences on Freezing Drizzle, Freezing Rain, and Ice Pellet Events. Wea. Forecasting. 15: pp. 485-508.

Bottyán, Z. (2011): Estimation of structural icing intensity and geometry of aircrafts during different conditions – a fixed-wing approach. Időjárás 115: pp. 275-288.

Bottyán, Z. – Wantuch, F. – Gyöngyösi, A. Z. – Tuba, Z. – Hadobács, K. – Kardos, P. – Kurunczi, R. (2013): Development of a complex meteorological support system for UAVs. World Academy of Science Engineering and Technology 76: pp. 1124-1129.

Bragg, M. B. – Broeren, A. P. – Blumenthal, L. A. (2005): Iced-airfoil aerodynamics. Prog. Aerospace Sci. 41: pp. 323-362.

Finstad, J. K. – Lozowski, E. P. – Gates, E. M. (1988): A computational investigation of water droplet trajectories. J. Atmos. Ocean. Tech. 5: pp. 160-170.

Fuchs, W. – Schickel, K. P. (1995): Aircraft icing in visual meterological conditions below low stratus clouds. Atmos. Res. 36: pp. 339-345.

Gent, R. W. – Dart, N. P. – Cansdale, J. T. (2000): Aircraft icing, Phil. Trans. R. Soc. Lond. A., 358: pp. 2873-2911.

Hansen, B. (2007): A fuzzy-logic based analog forecasting system for ceiling and visibility. Wea. Forecasting. 22: pp. 1319-1330.

Iijima, Y. – Shinoda, M. (2000): Seasonal Changes in the Cold-Air Pool Formation in a Subalpine Hollow, Central Japan. Int. J. Climatol. 20: pp. 1471-1483.

Jeck, R. (1998): A workable, aircraft-specific icing severity scheme. Appendix A. Preprints of AIAA-98-0094. 36th Aerospace Sciences Meeting and Exhibit. Reno, USA, pp. 1-12.

Jeck, R. (2002): Icing Design Envelopes (14 CFR Parts 25 and 29, Appendix C) Converted to a Distance-Based Format. Final Report of U.S. Department of Transportation Federal Aviation Administration Office of Aviation Research. Washington, USA, pp. 1-48.

Kunkel, B. A. (1971): Fog drop-size distributions measured with a laser hologram camera. J. Appl. Meteorol. 10: pp. 482-486.

Lankford, T. T. (2001): Aviation Weather Handbook. McGraw-Hill, New York.

Lozowski, E. P. – Stallabrass, J. R. – Hearty, P. F. (1983a): The icing of an unheated, non-rotating cylinder. Part I: A simulation model. Journal of Climate and Applied Meteorology 22: pp. 2053-2062.

Lozowski, E. P. – Stallabrass, J. R. – Hearty, P. F. (1983b): The icing of an unheated, non-rotating cylinder. Part II: Icing wind tunnel experiments. Journal of Climate and Applied Meteorology 22: pp. 2063-2074.

Ludlam, F. H. (1951): The heat economy of a rimed cylinder. Quarterly Journal of Royal Meteorological Society 77: pp. 663-666.

Makkonen, L. – Stallabrass, J. R. (1987): Experiments on the cloud droplet collision efficiency of cylinders. Journal of Climate and Applied Meteorology 26: pp. 1406-1411.

Mazin, I. P. – Korolev, A. V. – Heymsfield, A. – Isaac, G. A. – Cober, S. G. (2001): Thermodynamics of icing cylinder for measurements of liquid water content in supercooled clouds. J. Atmos. Ocean. Tech. 18: pp. 543-558.

Messinger, B. L. (1953): Equilibrium temperature of an unheated icing surface as a function of airspeed. J. Aeronaut. Sci. 20: pp. 29-41.

Skamarock, W. C. – Klemp, J. B. – Dudhia, J. – Gill, D. O. – Barker, D. M. – Wang, W. – Powers, J. G. (2005): A Description of the Advanced Research WRF Version 2. NCAR Technical. Note, Boulder, USA, pp. 1-88.

Szilder, K. – McIlwain, S. (2011): In-flight icing of UAVs – The influence of Reynolds number of the ice accretion process. SAE Technical Paper, 2011-01-2572, 2011, doi: 10.4271/2011-01-2572.

Tsao, J. C. – Anderson, D. N. (2005): Additional study of water droplet median volume diameter (MVD) effects on ice shape. NASA/CR-2005-213853 report, pp. 1-11.